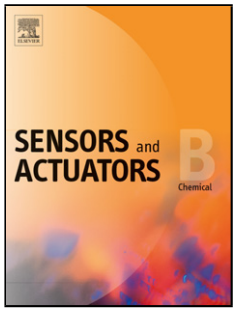

A Ratiometry-induced Successive Reusable Electrochemical Aptasensing Platform: Efficient Monitoring of Aflatoxin B1 in Peanut

Yuye Li (Investigation) (Data curation) (Writing - original draft), Dong Liu (Methodology) (Conceptualization) (Formal analysis) (Writing - review and editing), Chengxi Zhu (Resources) (Software), Meng Wang (Resources) (Software), Yang Liu (Resources) (Software), Tianyan You (Supervision) (Conceptualization) (Writing - review and editing)

PII: S0925-4005(20)31368-X

DOI: https://doi.org/10.1016/j.snb.2020.129021

Reference: SNB 129021

To appear in: *Sensors and Actuators: B. Chemical*

Received Date: 15 August 2020

Revised Date: 6 October 2020

Accepted Date: 7 October 2020

Please cite this article as: Li Y, Liu D, Zhu C, Wang M, Liu Y, You T, A Ratiometry-induced Successive Reusable Electrochemical Aptasensing Platform: Efficient Monitoring of Aflatoxin B1 in Peanut, *Sensors and Actuators: B. Chemical* (2020), doi: https://doi.org/10.1016/j.snb.2020.129021

A Ratiometry-induced Successive Reusable Electrochemical Aptasensing Platform: Efficient Monitoring of Aflatoxin B1 in Peanut

Yuye Li [a], Dong Liu [a, *], Chengxi Zhu [a], Meng Wang [b], Yang Liu [c], Tianyan You [a, *]

[a] *Key Laboratory of Modern Agricultural Equipment and Technology, Ministry of Education, School of Agricultural Engineering, Jiangsu University, Zhenjiang, Jiangsu 212013, China*

[b] *Beijing Research Center for Agricultural Standards and Testing, No. 9 Middle Road of Shuguanghuayuan, Haidian Dist. Beijing, 100097, China.*

[c] *College of Science and Engineering, James Cook University, Townsville, Queensland 4811, Australia*

*Corresponding author: Dong Liu E-mail: dongliu@ujs.edu.cn

Tianyan You E-mail: youty@ujs.edu.cn

Highlights

- The successive reusable electrochemical method was achieved on the basis of ratiometric strategy.
- A reusable electrochemical assay was developed for successive detection of AFB1 in peanut.
- The aptasensor showed enhanced analytical properties compared with sensors based on single-signal response mode.

Abstract

Currently, most reusable aptasensors rely on the reassembly of aptamers to regenerate the sensing interface. However, it remains challenging to achieve successive aptasensor reusability. Herein, for the first time, we demonstrate that a ratiometric strategy endows the electrochemical aptasensor high reusability to realize the successive detection of aflatoxin B1 (AFB1). The model sensing interface used thionine (THI)-graphene nanocomposite and ferrocene (Fc)-labeled aptamer to output current signals (I_{THI} and I_{Fc}). For analysis, the specific recognition of AFB1 by aptamers caused it to strip from the electrode, and the value of I_{THI}/I_{Fc} varied linearly with AFB1 concentration over the 0.01-100 ng mL^{-1} range. This relationship also worked when using a single sensor for multiple successive testing but completely failed with I_{THI} or I_{Fc} alone. This unique successive reusability was ascribed to the

ratiometric strategy capable of eliminating the environmental influence on both signals. The feasibility of the proposed aptasensor was validated by applying it to the successive detection of AFB1, which showed excellent accuracy and reliability compared with the official method, i.e., standard high-performance liquid chromatography-fluorescence (HPLC-FL). This successive reusable electrochemical aptasensing platform can be universal for advanced analysis, and it promotes the practical applications of aptasensors particularly in the field of rapid assays.

Keywords: Ratiometry; Electrochemical aptasensor; Successive reusability; Aflatoxin B1

1. Introduction

Aflatoxin B1 (AFB1) is one of the most toxic mycotoxins produced by fungi and has caused widespread concern due to its ability to bind to the cellular DNA. This increases the risk of developing human liver cancer (Hu et al., 2015; Shephard, 2008; Xie et al., 2017). Even worse, AFB1 contamination can occur in various agricultural products because of the inevitable fungal growth (Bayram et al., 2017; Li et al., 2009). The standard method for AFB1 analysis currently relies on high performance liquid chromatography-fluorescence (HPLC-FL). Despite the high sensitivity and accuracy, the technique requires specialized operators and expensive facilities that are unsuitable for routine measurement (Machado Trombete et al., 2014). Therefore, alternative methods that can realize accurate detection of AFB1 without relying on conventional laboratory resources are highly desirable.

Electrochemical sensors have been extensively exploited due to their fast response time and ease of miniaturization, which present great application prospects in the fields of environmental monitoring and food safety(Castillo et al., 2015; Rackus et al., 2015; Wang et al., 2018; Wu et al., 2017; Wu et al., 2019). Recently, biological recognition elements such as aptamers and antibodies with high affinity for targets have attracted considerable interest in the development of electrochemical sensing platforms. For AFB1 analysis, many electrochemical aptasensors with excellent sensitivity and selectivity have been constructed by taking advantage of the specific recognition of the corresponding aptamer (Goud et al., 2017; Wang et al., 2018; Wu et al., 2019). Their working principles are mainly on account of single-signal detection

type, which outputs the response signal associated with the conformational change of electroactive probe-labeled aptamer. Nevertheless, the analytical performance of these aptasensors can be easily affected by environmental factors (such as temperatures, analyte and analyte) and electrode surface state, which makes it extremely challenging to retain their accuracy in various application scenarios (Li et al., 2019; Wang et al., 2019b).

Ratiometry has emerged as a tool to achieve superior accuracy and reliability of aptasensors because of its self-referencing ability (Jin et al., 2017; Wang et al., 2019b; Yang et al., 2018; Zhu et al., 2019). Unlike the single-signal detection mode, ratiometric strategies utilize the ratio of two dependent signals to reduce error (Zhu et al., 2020). For example, semiconductor quantum dots can be a ratiometric signal generator to normalize environmental and electrode variables (Wang et al., 2019a). Meanwhile, this strategy could give aptasensors other attractive features such as programmable sensitivity by regulating the ratiometric signal values (Li et al., 2020). Thus, coupling the electrochemical techniques with ratiometry can be extremely advantageous over conventional analytical methods for accurate analysis of AFB1 in agricultural products.

Although many efforts have been made for the development of disposable electrochemical aptasensors due to their fast response and easy operation (Li et al., 2018), reusable aptasensors with high efficiency and low cost have attracted increasing attention over the last few years. For example, electrochemical Hg^{2+} aptasensors based on thymine-Hg^{2+}-thymine interaction can be regenerated by

incubating the aptasensor with cysteine for two hours. This is cost-effective and environment-friendly (Zeng et al., 2017). Generally, the reassembly of aptamers at the electrode surface is required to regenerate the aptasensors due to high affinity binding between aptamers and targets (Hu et al., 2014; Song et al., 2019; Tee et al., 2015; Wang et al., 2019c). The typical working principle of these reusable aptasensors is as follows: the specific recognition of a target by an aptamer leads to its stripping from the aptasensor leaving the complementary DNA on the electrode. The aptasensor can then be regenerated by incubation with the aptamer again (Li et al., 2017; Yu & Lai, 2018). Since this method is time-consuming, an efficient platform that enables the reusability without any pre-treatment procedures is highly desirable.

Here, we report a ratiometry-induced electrochemical aptasensor that can be successively reused for AFB1 detection with high accuracy. The sensing interface was fabricated by thionine (THI)-functionalized reduced graphene oxide and ferrocene-labeled aptamer (Fc-apt) whose current responses changed with the stripping of Fc-apt-AFB1, while the current response ratio (I_{THI}/I_{Fc}) was linearly related to the concentration of AFB1 leading to ratiometric analysis of AFB1 without interference from environmental conditions or electrode states. Furthermore, the AFB1 aptasensor can be reused for multiple tests with good linearity and fast response, which makes it attractive for practical applications. The applicability of the proposed ratiometric strategy was also investigated, and demonstrating good reliability with superior efficiency for HPLC-FL.

2. Experimental

2.1. Materials and Instrumentation

The AFB1 aptamer (*5'-Fc-GTTGGGCACGTGTTGTCTCTCTGTGTCTCGTGCCC TTCGCTAGGCCCACA-Fc-3'*, Fc-apt) (Castillo et al., 2015) was provided by Sangon Biotech Co., Ltd (Shanghai, China). Reduced graphene oxide (rGO, XFNANO Inc), thionine (THI, 100%, Alfa Aesar), chitosan (CS, Aladdin) were used. Aflatoxin B1 (AFB1, 98%), zearalenone (ZEN, 98%), aflatoxin B2 (AFB2, 98%), ochratoxin (OTA, 98%), fumonectin B1 (FB1, 96%) were purchased from J&K Chemicals.

A Hitachi SU8020 scanning electron microscope (Hitachi, Japan) was utilized to record the structures of the prepared nanocomposite. The electrochemical experiments were carried out on a CHI 750E electrochemical workstation (Chenhua, China). Details of other reagents and characterization are provided in Supporting Information.

2.2. Electrochemical analysis

2.2.1 Fabrication of aptasensor

Bare glassy carbon electrode (GCE, Φ: 3 mm) was polished carefully with alumina powder (0.3 μm, 0.05 μm), and then cleaned with ethanol and water to remove the residual alumina powder. The prepared THI-rGO (Zhao et al., 2015) and CS (0.5%, pH 5) solutions were successively modified on GCE. Then, Fc-apt (2.0 μM, 6 μL) was assembled on the GCE. After washing, the obtained aptasensor was stored in the dark (4 °C) before use.

2.2.2 The disposable aptasensor detect AFB1

Standard solutions with different concentrations of AFB1 were prepared with 0.1 M phosphate buffer solution (PBS, pH 7.0). For analysis, 6 μL of standard solution was

dropped on the freshly aptasensor and incubated for 1 h before rinsed with PBS. Then, this aptasensor was applied to alternating current voltammetry measurement with a potential range of -0.4 V to 0.7 V in 0.1 M PBS (pH=7.0).

2.2.3 The successive reusable aptasensor detect AFB1

To access the successive reusability, a single aptasensor was repeatedly used for the detection of AFB1. As a proof-of-concept experiment, 5 of 1 ng ml^{-1} AFB1 solution were successively analyzed by using a single aptasensor, and only the PBS washing was required after every detection. All parameters used in the electrochemical testing were identical with those in Section 2.2.2.

2.3 Pretreatment process of peanut sample

Peanut samples were pretreated according to the previous report, and the details are provided in Supporting Information (Li et al., 2020).

2.4 Monitoring the moldy process of peanut kernel and crushed peanut

The proposed aptasensor was used to monitor the moldy process of peanut products. Peanut kernel sample was purchased from the local market (Zhenjiang, China), and crushed peanut sample was prepared by comminuting peanut kernel. In the test, these two samples were stored in a humid environment for 14 day to get mildewed. During the storage, their morphologies were recorded every day, and the concentrations of AFB1 in these two samples were analyzed by using the proposed aptasensor. The pretreatment process of the moldy peanut kernel and crushed peanut was as follows. After adding 20 mL of 60% methanol aqueous solution, the sample was ultrasonic extraction for 60 min and then centrifuged at 8000 rpm for 15 min. The

supernatant was then treated with 0.22 μm filter to remove impurities, and finally the sample solution of AFB1 was obtained.

3. Results and discussion

3.1. Assay principle

The reusable electrochemical aptasensing system described here achieves rapid detection of AFB1 with high accuracy by avoiding regeneration procedures to realize successive analysis. Scheme 1 shows that the proposed aptasensor was fabricated by assembling THI-rGO nanocomposite and Fc-apt on the electrode to output I_{THI} and I_{Fc} signals. During the analysis, AFB1 could be specifically recognized by Fc-apt, which was stripped from the GCE leading to a decrease in I_{Fc}. Since the I_{THI} value remained constant, the ratio of I_{THI} to I_{Fc} (I_{THI}/I_{Fc}) was found to be linear with the logarithm of AFB1 concentration (C_{AFB1}) with a corresponding regression equation of $I_{THI}/I_{Fc} = 0.16\log C_{AFB1} + 1.33$. After the first measurement, the remaining aptamers on the electrode could still recognize AFB1 followed by stripping from the electrode to ratiometrically detect the analyte. This aptasensor could be reusable for multiple measurements. During the successive analysis, I_{THI} or I_{Fc} varied irregularly for the changes of environmental conditions and electrode status; however, I_{THI}/I_{Fc} still obeyed the above-mentioned linear relationship between I_{THI}/I_{Fc} and C_{AFB1} indicating the feasibility of successive analysis.

Scheme 1

3.2. Characterization of modified aptasensor

The THI-rGO was prepared according to our previous report (Li et al., 2020). The

scanning electron microscope (SEM) and other characterizations confirmed the successful preparation of THI-rGO (Fig. 1A and S1).

The proposed aptasensor was then constructed, and the fabrication process was characterized using cyclic voltammetry (CV) and EIS. Fig. 1B shows a reversible redox peak assigned to $[Fe(CN)_6]^{3-/4-}$ (curve a) on bare GCE. The following modification of THI-rGO leads to an increased peak current for the enlarged surface area (curve b) while anchoring Fc-apt significantly reduces the peak current (curve d) due to the steric effect. A significant increase in peak currents can be observed when AFB1-Fc-apt was stripped from the GCE surface (curve e). EIS was then performed to assess different stages of aptasensor construction in terms of charge transfer resistance (R_{et}) (Fig. 1C). THI-rGO/GCE (curve b) shows a reduced R_{et} compared with GCE (curve a), An obvious increase in R_{et} is recorded at Fc-apt/THI-rGO/GCE (522 Ω, curve d). Subsequently, the response principle of the aptasensor for AFB1 was investigated. The recorded R_{et} reduces to 337 Ω (curve e) after incubating AFB1 at the Fc-apt/THI-rGO/GCE. These data confirm the stripping of the formed Fc-apt-AFB1 complex as expected. In summary, the EIS data are consistent with the CV confirming the success of each step of material modification on the sensing interface.

Fig. 1

Next, experimental parameters including reaction time, concentration and incubation time of Fc-apt were optimized in detail. Fig. S2A shows the variance of I_{Fc} for Fc-apt incubation time. As the Fc-apt incubation time increases from 6 to 10 h, the I_{Fc} increases gradually and levels off at 12 h due to the poor conductivity of the DNA

layer. Therefore, 12 h was employed in the subsequent experiments. The effect of Fc-apt concentration I_{Fc} was estimated. Fig. S2B shows that the I_{Fc} increases with the concentration of Fc-apt from 0.8 to 2.0 μM, and then decreases when the concentration is over 2.0 μM. This is attributed to the increase in Fc-apt density that leads to steric hindrance and electrostatic repulsion. Thus, 2.0 μM Fc-apt was used in the subsequent experiments. Fig. S2C shows that the I_{Fc} decreases with incubation time of the target AFB1 from 0.33 to 1 h due to the peeling of AFB1-Fc-apt. There was no significant change after the time reached 1 h. We found that the incubation time of the target AFB1 was 1.33 h.

3.3. Analytical properties of the aptasensor

To estimate the analytical properties, the fabricated aptasensor was used to analyze standard solutions containing different concentrations of AFB1 (C_{AFB1}). The experiments were performed with two strategies: 1) the disposable mode that used different aptasensors for solutions with various C_{AFB1} and 2) the successive reusable mode that used a single aptasensor for solutions with various C_{AFB1}.

3.3.1. Disposable mode

The analytical properties of the proposed electrochemical aptasensor with a disposable-mode were evaluated under optimal conditions. The I_{THI} remains stable and I_{Fc} decreases as the AFB1 concentration (C_{AFB1}) increases (Fig. 1D). The I_{THI}/I_{Fc} value exhibits a linear correlation with the C_{AFB1} from 0.01 to 100 ng mL^{-1}. And the limit of detection (LOD) of the aptasensor is down to 0.01 ng mL^{-1} (Fig. 1E). The corresponding regression equation is $I_{THI}/I_{Fc} = 0.16 \log C_{AFB1} + 1.33$ with a

regression coefficient (R^2) of 0.998.

In comparison, the analytical performance of the individual signal I_{Fc} of the aptasensor was also investigated. The result in Fig. 1F shows that I_{Fc} is logarithmically related to C_{AFB1} with a regression equation of $I_{Fc} = -0.1\log C_{AFB1} + 0.962$ (R^2=0.984). The value of R^2 for the ratiometric method is much larger than that for a single-signal method to get the same linear range demonstrating the superior accuracy of the ratiometric method.

3.3.2. Successive reusable mode

The reusability of the fabricated aptasensor was measured in terms of successive detection of AFB1 (1 ng mL^{-1}) for five times. The resulting ACV data (Fig. 2A) reveals that both I_{Fc} and I_{THI} show erratic decline as successive measurements due to the changes in the structural dynamics of the solid-liquid interfaces (Su et al., 2020); however, their current intensity ratio, I_{THI}/I_{Fc}, regularly increases (Fig. 2A insert). Substituting the I_{THI}/I_{Fc} (1.32, 1.38, 1.40, 1.42, 1.45) experimental data into the regression equation of $I_{THI}/I_{Fc} = 0.16\log C_{AFB1} + 1.33$ of the disposable electrochemical aptasensor indicates that the detected AFB1 concentration is basically consistent with the theoretical value. The relationship between I_{THI}/I_{Fc} and C_{AFB1} follows the formula of $\log_{10}\sum_{i=1}^{5} C_{AFB1} = (I_{THI}/I_{Fc} - 1.33)/0.16$ (Fig. 2B insert). The recovery for the detection of 1 ng mL^{-1} AFB1 is between 85% and 106% (Table 1) with a relative standard deviation (RSD) of less than 1.1% (Fig. S3A). The RSD for five replicate rounds of detection is 9.61% indicating the high accuracy. To further validate the reusability, experiment that used a single aptasensor for the detection of

AFB1 with different concentrations (0.01, 0.1, 1, 5, and 20 ng mL^{-1}) was performed (Fig. S3B). And the recoveries are between 95% and 115%, confirming the high reliability (Table S1). Thus, all these results have demonstrated the attracting successive reusability of the as-developed aptasensor. Noteworthy, the utilization of a single aptasensor for successive analysis of samples with close concentrations (i.e., same batch of samples) and varied ones (i.e., different batches of samples) suggests the applicability of aptasensor in various scenarios. Compared to previous reports, the developed aptasensor here shows the following merits. Firstly, such aptasensor fulfills the successively multiple detection without any regeneration process, providing a better assay efficiency. Secondly, the successive reusable strategy can simplify the experimental process and improve the reliability of the analytical results. Finally, such unique reusability derived from ratiometry has a potential to eliminate environmental influences (e. g., ionic strength, temperature, pH) and expand the application of aptasensor.

Fig. 2

The working principle of successive reusability of the aptasensor was further investigated via SEM and EIS. Fig. 2C presents SEM images: The morphology of the Fc-apt/CS/THI-rGO/GCE displays no obvious change after five rounds of successive detection. The Fc-apt at the aptasensor surface cannot be observed. The CS/THI-rGO/GCE sensing interface is relatively stable due to the fixation of the CS membrane. Meanwhile, the recorded R_{et} decreases with successive use of the aptasensor due to the reduced amount of Fc-apt (Fig. 2D). We then proceeded to

research the correlation between R_{et} and detection of 1 ng mL^{-1} AFB1 for five times. The result is shown in Fig. 2E; there is a linear relationship between R_{et} and the number of successive detections. The ΔR_{et} was used to analyze the varieties of the aptasensing interface after each successive detection, and Fig. 2F indicates that the aptasensor for each successive detection remains relatively constant. These observations are attributed to the successive reusability of the aptasensor deriving from the Fc-apt stripping-based response mode.

Table. 1

In summary, Table S2 compares the analytical performance for AFB1 analysis between the proposed aptasensor and published studies. Our system offers the lowest LOD versus other single-signal sensors. While the LOD of our aptasensor is slightly higher than the reported ratiometric sensor, it also has a wider linear range. It is worth noting that the aptasensing system is far more efficient because of its successive reusable performance for the AFB1 analysis.

Table. 2

3.3.3. Selectivity, reproducibility, and stability

The selectivity of the aptasensor was assessed by investigating its response to potential interferents, including AFB2, FB1, ZEN and OTA. In these experiments, the concentration of interferents (10 ng mL^{-1}) were 20-fold higher than that of 0.5 ng mL^{-1} AFB1. And the selectivity evaluation is shown in Fig. S4A. In contrast to the I_{THI}/I_{Fc} of AFB1 and mixed solution containing AFB1, a response lower than the blank was observed upon addition of AFB2, FB1, ZEN, OTA, and the mixed solution. This

phenomenon is ascribed to the absorption of these interfering substances at the electrode surface impeding the electron transfer of THI (Wang et al., 2018), which demonstrates the favorable selectivity of the aptasensor for AFB1 analysis.

Fig. 3

The reproducibility was then evaluated by measuring six different aptasensors in the presence of 0.5 ng mL^{-1} AFB1. The calculated RSD 0.64% indicates high reproducibility (Fig. S4B). Aptasensors were kept at 4 °C for 7 days, and the I_{THI}/I_{Fc} exhibits only a 3.16% decrease suggesting high stability of the aptasensor (Fig. S4C).

3.4. Analysis of the spiked peanut samples

To assess the practical applicability of the proposed aptasensor, a standard addition experiment was performed with peanut samples (obtained from Jiangsu supermarket). Table 2 shows the results for peanut samples spiked with AFB1 at 0.05, 0.5 and 5 ng mL^{-1} by using the disposable aptasensor, offering the recoveries ranging in 94%-116%. Then, the successive reusable aptasensor was applied to analyze three samples with different C_{AFB1}, and the resultant recoveries varied from 88% to 104%.

The HPLC-FL method was introduced to verify the reliability of the aptasensor for real sample analysis. The better recoveries indicate that the proposed aptasensor can be used for the detection of real sample. The aptasensor could detect AFB1 at a concentration of 0.05 ng mL^{-1}, but the detection limit of HPLC-FL is 0.1 ng mL^{-1} confirming the potential use of the aptasensor in real samples.

Table. 3

3.5. Monitoring AFB1 in the mildew process of peanut kernel and crushed peanut

We next used the sensor to measure AFB1 in peanut kernel and crushed peanut (without AFB1 before mildew process) during the 14-day mildew process in a humid environment.

Fig. 4

As shown in Fig. 3, there was an obvious surface change in the peanut kernels and peanut debris on the 4^{th} day by naked eye. From the 4^{th} to 8^{th} day, the mildew growth rate of peanut kernels increased rapidly while the mildew process of crushed peanut showed a straight upward trend from the 3^{rd} to 6^{th} day. After the 9^{th} day, there was no distinguishable change in the rate of mold production and mildew color in either peanut samples. The results show that the whole mildew processes of peanut kernel and crushed peanut are similar. However, while it is convenient to visually monitor mildew on peanut, it is difficult to observe when the mildew is in the initial state.

In fact, the presence of AFB1 was already confirmed on the 3^{rd} day via the proposed aptasensor. After the incubation for 48 hours, the AFB1 contents were detected at 0.01 and 0.03 ng mL^{-1} in the moldy peanut (Fig. 3). The content of AFB1 in peanut kernels was 4 ng mL^{-1} on the 7^{th} day while the content in crushed peanut reached 20 ng mL^{-1} on the 6^{th} day. This result indicates that crushed peanut mildews faster than peanut kernels. Subsequently, 60 ng mL^{-1} and 70 ng mL^{-1} AFB1 were detected in peanut kernels and crushed peanut, respectively, on the 10^{th} day. These values remained relatively stable in the following days.

These results demonstrate that aptasensor could provide an earlier warning of mildew in peanut compared with naked-eye observations. The HPLC-FL method was

employed to verify the concentration of AFB1 during the mildew of peanut kernel and shredded peanut at 4^{th}, 6^{th}, 8^{th} and 10^{th} day. And the results were summarized in Table S3, which illuminated that these two methods had good agreement, suggesting the high reliability of our developed aptasensor in moldy process analysis. More importantly, our aptasensor can achieve quantitative detection of AFB1 during the mildew process with high convenience and accuracy. This is likely to be highly favorable in studies of dynamic change or mildew.

4. Conclusion

In this work, a ratiometry-induced successive reusable aptasensor was fabricated for the efficient detection of AFB1 via THI-rGO as a reference signal and Fc as a response signal. The proposed aptasensor has some attractive features. First, unlike a single-signal detection method, dual-signal detection can be cross-referenced. This not only greatly improves the detection reliability and accuracy, but also lays the foundation for building a successively reusable aptasensor. Second, the proposed reusable aptasensor could improve the efficiency and utilization of the aptamer. Finally, the aptasensor offers a relatively low LOD (0.01 ng mL^{-1}) for AFB1 detection.

CRediT authorship contribution statement

Yuye Li: Investigation, Data curation, Writing - original draft. **Dong Liu**: Methodology, Conceptualization, Formal analysis, Writing - review & editing. **Chengxi Zhu**: Resources, Software. **Meng Wang**: Resources, Software. **Yang Liu**:

Resources, Software. **Tianyan You**: Supervision, Conceptualization, Writing - review & editing.

Declaration of interest statement

We declare that we have no known competing financial interests or personal relationships that could have appeared to influence the work reported in this paper.

Acknowledgments

The proposed work was sustained by National Natural Science Foundation of China (No. 61901193, 22074055), Priority Academic Program Development of Jiangsu Higher Education Institutions, the Innovation/Entrepreneurship Program of Jiangsu Province, Six Categories Talent Peak of Jiangsu Province (No. NY-011), Postgraduate Research & Practice Innovation Program of Jiangsu Province (KYCX20_3087), Natural Science Foundation of Jiangsu Province (No. BK20160490), Zhenjiang Key Laboratory of Advanced Sensing Materials and Devices (No. SS2018001).

References

Bayram, E., Yilmaz, E., Uzun, L., Say, R., Denizli, A., 2017. Food Chem. 221, 829-837.

Castillo, G., Spinella, K., Poturnayová, A., Šnejdárková, M., Mosiello, L., Hianik, T., 2015. Food Control 52, 9-18.

Chen, L., Wen, F., Li, M., Guo, X., Li, S., Zheng, N., Wang, J., 2017. Food Chem. 215, 377-382.

Goud, K.Y., Hayat, A., Catanante, G., M, S., Gobi, K.V., Marty, J.L., 2017. Electrochim. Acta 244, 96-103.

Hu, J., Yu, Y., Brooks, J.C., Godwin, L.A., Somasundaram, S., Torabinejad, F., Kim, J., Shannon, C., Easley, C.J., 2014. J. Am. Chem. Soc. 136, 8467-8474.

Hu, Z., Lustig, W.P., Zhang, J., Zheng, C., Wang, H., Teat, S.J., Gong, Q., Rudd, N.D., Li, J., 2015. J. Am. Chem. Soc. 137, 16209-16215.

Jin, H., Gui, R., Yu, J., Lv, W., Wang, Z., 2017. Biosens. Bioelectron. 91, 523-537.

Li, J., He, G., Wang, B., Shi, L., Gao, T., Li, G., 2018. Anal. Chim. Acta 1026, 140-146.

Li, L.L., Li, M.M., Wang, W.W., Zhang, Q., Liu, D.Y., Li, X.H., Jiang, H., 2017. Sensors 17, 992.

Li, P., Zhang, Q., Zhang, W., 2009. TrAC Trends in Anal. Chemi. 28, 1115-1126.

Li, Y., Chang, Y., Ma, J., Wu, Z., Yuan, R., Chai, Y., 2019. Anal. Chem. 91, 6127-

6133.

Li, Y.Y., Liu, D., Zhu, C.X., Shen, X.L., Liu, Y., You, T.Y., 2020. J. of Hazard. Mater. 387, 122001.

Machado Trombete, F., de Ávila Moraes, D., Duarte Porto, Y., Barbosa Santos, T., Maria Direito, G., Elias Fraga, M., Saldanha, T., 2014. J. of Food Nutr. Res. 2, 671-674.

Rackus, D.G., Shamsi, M.H., Wheeler, A.R., 2015. Chem. Soc. Rev. 44, 5320-5330.

Seok, Y., Byun, J.Y., Shim, W.B., Kim, M.G., 2015. Anal. Chim. Acta 886, 182-187.

Shephard, G.S., 2008. Chem. Soc. Rev. 37, 2468-2477.

Shim, W.B., Mun, H., Joung, H.A., Ofori, J.A., Chung, D.H., Kim, M.G., 2014. Food Control 36, 30-35.

Song, J., Li, S., Gao, F., Wang, Q., Lin, Z., 2019. Chem. Commun. 55, 905-908.

Su, H., Zhou W.L., Zhang, H., Zhou, W., Zhao, X., Li, Y., Liu, M.H., Cheng W., Liu, Q.H., 2020. J. Am. Chem. Soc. 142, 12306-12313.

Tee, S.Y., Ye, E., Pan, P.H., Lee, C.J., Hui, H.K., Zhang, S.Y., Koh, L.D., Dong, Z., Han, M.Y., 2015. Nanoscale 7, 11190-11198.

Wang, C., Qian, J., An, K., Lu, X., Huang, X., 2019a. Analyst 144, 4772-4780.

Wang, C., Qian, J., An, K., Ren, C., Lu, X., Hao, N., Liu, Q., Li, H., Huang, X., Wang, K., 2018. Biosens. Bioelectron. 108, 69-75.

Wang, X., Liu, G., Qi, Y., Yuan, Y., Gao, J., Luo, X., Yang, T., 2019b. Anal. Chem. 91, 12006-12013.

Wang, Z., Wang, X., Zhu, X., Lv, J., Zhang, J., Zhu, Q., Dai, Z., 2019c. Sens.

Actuators B 285, 438-444.

Wu, L., Ding, F., Yin, W., Ma, J., Wang, B., Nie, A., Han, H., 2017. Anal. Chem. 89, 7578-7585.

Wu, S.S., Wei, M., Wei, W., Liu, Y., Liu, S., 2019. Biosens. Bioelectron. 129, 58-63.

Xie, G., Zhu, M., Liu, Z., Zhang, B., Shi, M., Wang, S., 2017. Food Agr. Immunol. 29, 564-576.

Yang, T., Yu, R., Yan, Y., Zeng, H., Luo, S., Liu, N., Morrin, A., Luo, X., Li, W., 2018. Sens. Actuators B 274, 501-516.

Yu, Z.G., Lai, R.Y., 2018. Talanta 176, 619-624.

Zeng, G., Zhang, C., Huang, D., Lai, C., Tang, L., Zhou, Y., Xu, P., Wang, H., Qin, L., Cheng, M., 2017. Biosens. Bioelectron. 90, 542-548.

Zhang, X., Li, C.R., Wang, W.C., Xue, J., Huang, Y.L., Yang, X.X., Tan, B., Zhou, X.P., Shao, C., Ding, S.J., Qiu, J.F., 2016. Food Chem. 192, 197-202.

Zhao, Z., Chen, H., Ma, L., Liu, D., Wang, Z., 2015. Analyst 140, 5570-5577.

Zhu, C.X., Liu, D., Li, Y.Y., Shen, X.L., Li, L.B., Liu, Y., You, T.Y., 2019. Curr. Opin. Electrochem. 17, 47-55.

Zhu, C.X., Liu, D., Li, Y.Y., Shen, X.L., Ma, S., Liu, Y., You, T.Y., 2020. Biosens. Bioelectron. 150, 111814.

Figure Captions

Scheme 1. Schematic illustration of the successive reusable assay for AFB1 detection.

Fig. 1. (A) The SEM image of THI-rGO. (a) Bare GCE, (b) GCE/THI-rGO, (c) GCE/THI-rGO/CS, (d) GCE/THI-rGO/CS/Fc-apt, and (e) GCE/THI-rGO/CS/Fc-apt/AFB1 were compared using (B) CVs and (C) EIS. Inset 1: Magnified diagram of (a) bare GCE, (b) GCE/THI-rGO, (c) GCE/THI-rGO/CS. Inset 2: Equivalent circuit. R_s: the resistance of the electrolyte solution; Q: constant phase element; R_{et}: electron transfer resistance; Z_w: Warburg impedance. (D) Signal responses for detecting different concentrations AFB1 (0.01, 0.05, 0.1, 0.5, 5, 20, and 100 ng mL^{-1}) in 0.1 M PBS (pH=7.0). (E) Logarithmic dependence of the ACV peak current ratio of I_{THI}/I_{Fc} upon the concentration of AFB1. (F) Logarithmic dependence of Fc peak current signal upon the concentration of AFB1.

Fig. 2. (A) ACV responses of the aptasensor during five successive rounds of sensing (C1-C5) for AFB1 detection with concentrations of 1 ng mL^{-1}; 1.32, 1.38, 1.40, 1.42, and 1.45 are the values of I_{THI}/I_{Fc}, respectively. (B) The calibration curve for AFB1 determination of the disposable aptasensor, and the I_{THI}/I_{Fc} responses (1.32, 1.38, 1.40, 1.42, and 1.45). (C) SEM and (D) EIS of the aptasensor during these detection replicates. (E) Relationship between the analysis replicate and EIS data. (F) Changes in EIS of the sensing interface after each successive detection of the aptasensor; inset illustrates stripping of AFB1-Fc-apt.

Fig. 3. Monitoring AFB1 produced during the mildew process in (A) peanut kernel and (B) shredded peanut. The abscissa represents the time, and the ordinate represents the measured AFB1 levels. Inset: pictures of mildew in peanut kernel and shredded peanut.

Scheme 1

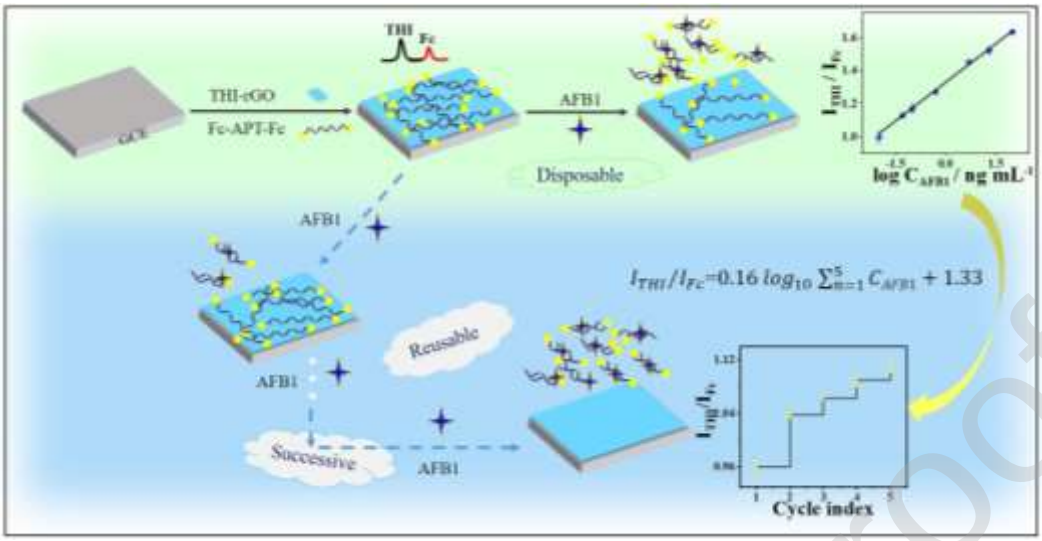

Fig. 1

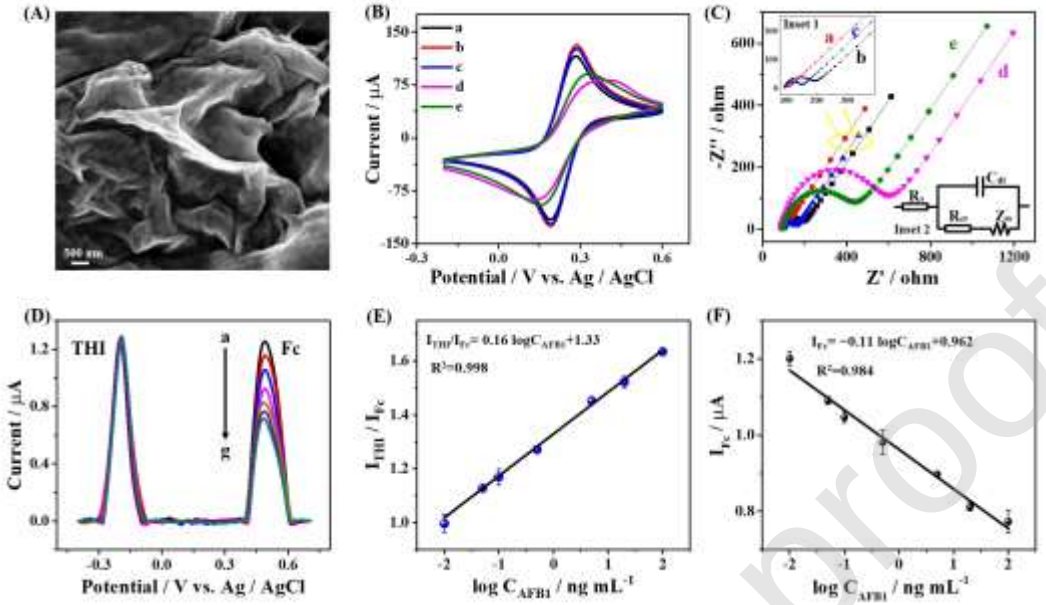

Fig. 2

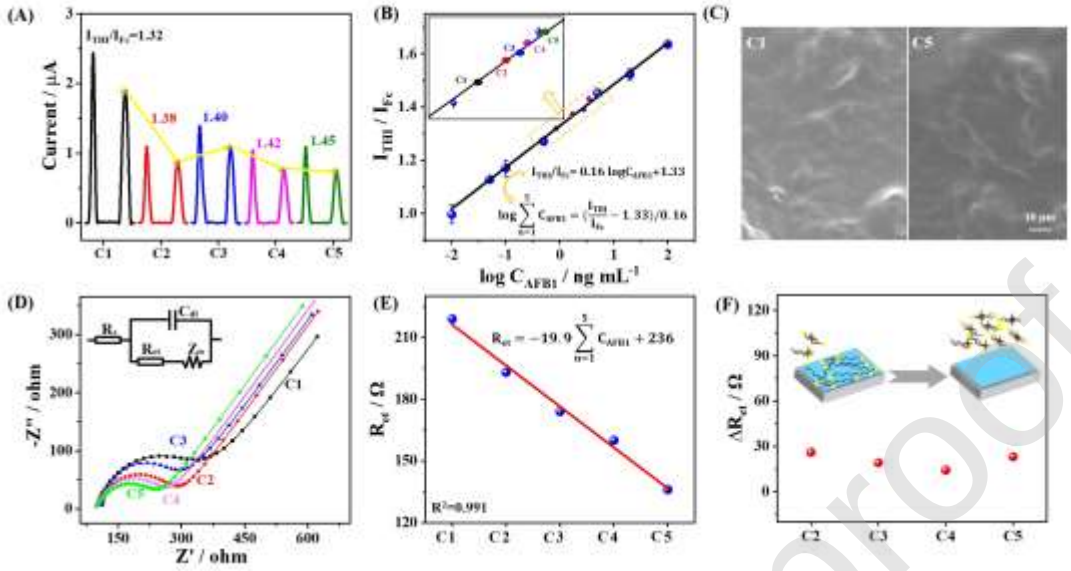

Fig. 3

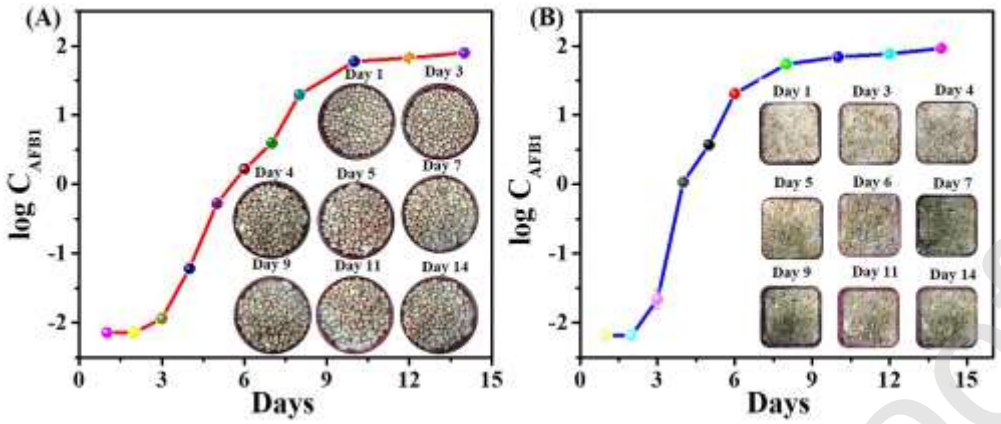

Table 1

Successive times	C_{AFB1} (ng mL^{-1})	Detected (ng mL^{-1})	Recovery (%)
1	1	0.94	94
2	1	0.97	97
3	1	0.86	86
4	1	0.85	85
5	1	1.06	106
RSD (%)	9.61		

Table 2

Sample	C_{AFB1} (ng mL^{-1})	Disposable mode			Successive reusable mode			HPLC-FL	
		Detected (ng mL^{-1})	RSD (%)	Recovery (%)	Detected (ng mL^{-1})	RSD (%)	Recovery (%)	Detected (ng mL^{-1})	Recovery (%)
1	0	ND	--	--	ND	--	--	--	--
2	0.05	0.048	6	96	0.044	6.5	88	--	--
3	0.5	0.58	5.5	116	0.504	3.2	101	0.516	103
4	5	4.7	6.8	94	5.18	1.7	104	4.98	99